

# UNIVERSITY OF BIRMINGHAM

## Research at Birmingham

### Detection of brake wear aerosols by aerosol time-of-flight mass spectrometry

Beddows, David; Dall'Osto, Manuel; Olatunbosun, Oluremi; Harrison, Roy

DOI:

[10.1016/j.atmosenv.2016.01.018](https://doi.org/10.1016/j.atmosenv.2016.01.018)

License:

Creative Commons: Attribution-NonCommercial-NoDerivs (CC BY-NC-ND)

*Document Version*

Peer reviewed version

*Citation for published version (Harvard):*

Beddows, D, Dall'osto, M, Olatunbosun, O & Harrison, RM 2016, 'Detection of brake wear aerosols by aerosol time-of-flight mass spectrometry', *Atmospheric Environment*, vol. 129, pp. 167-175.  
<https://doi.org/10.1016/j.atmosenv.2016.01.018>

[Link to publication on Research at Birmingham portal](#)

**Publisher Rights Statement:**

After an embargo period this document is subject to a Creative Commons Non-Commercial No Derivatives license

Checked Feb 2016

**General rights**

Unless a licence is specified above, all rights (including copyright and moral rights) in this document are retained by the authors and/or the copyright holders. The express permission of the copyright holder must be obtained for any use of this material other than for purposes permitted by law.

- Users may freely distribute the URL that is used to identify this publication.
- Users may download and/or print one copy of the publication from the University of Birmingham research portal for the purpose of private study or non-commercial research.
- User may use extracts from the document in line with the concept of 'fair dealing' under the Copyright, Designs and Patents Act 1988 (?)
- Users may not further distribute the material nor use it for the purposes of commercial gain.

Where a licence is displayed above, please note the terms and conditions of the licence govern your use of this document.

When citing, please reference the published version.

**Take down policy**

While the University of Birmingham exercises care and attention in making items available there are rare occasions when an item has been uploaded in error or has been deemed to be commercially or otherwise sensitive.

If you believe that this is the case for this document, please contact [UBIRA@lists.bham.ac.uk](mailto:UBIRA@lists.bham.ac.uk) providing details and we will remove access to the work immediately and investigate.

# Accepted Manuscript

Detection of brake wear aerosols by aerosol time-of-flight mass spectrometry

D.C.S. Beddows, M. Dall'Osto, O.A. Olatunbosun, Roy M. Harrison

PII: S1352-2310(16)30026-7

DOI: [10.1016/j.atmosenv.2016.01.018](https://doi.org/10.1016/j.atmosenv.2016.01.018)

Reference: AEA 14398

To appear in: *Atmospheric Environment*

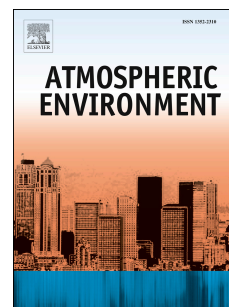
Received Date: 1 September 2015

Revised Date: 7 January 2016

Accepted Date: 9 January 2016

Please cite this article as: Beddows, D.C.S., Dall'Osto, M., Olatunbosun, O.A., Harrison, R.M., Detection of brake wear aerosols by aerosol time-of-flight mass spectrometry, *Atmospheric Environment* (2016), doi: 10.1016/j.atmosenv.2016.01.018.

This is a PDF file of an unedited manuscript that has been accepted for publication. As a service to our customers we are providing this early version of the manuscript. The manuscript will undergo copyediting, typesetting, and review of the resulting proof before it is published in its final form. Please note that during the production process errors may be discovered which could affect the content, and all legal disclaimers that apply to the journal pertain.



1  
2  
3  
4  
5 **DETECTION OF BRAKE WEAR AEROSOLS BY**  
6 **AEROSOL TIME-OF-FLIGHT MASS**  
7 **SPECTROMETRY**

8  
9  
10 **D.C.S. Beddows<sup>1</sup>, M. Dall'Osto<sup>2</sup>,**  
11 **O.A. Olatunbosun and Roy M. Harrison<sup>1\*†</sup>**

12  
13  
14 **<sup>1</sup>Division of Environmental Health and Risk Management**  
15 **School of Geography, Earth and Environmental Sciences**  
16 **University of Birmingham, Edgbaston, Birmingham, B15 2TT**  
17 **United Kingdom**

18  
19  
20 **<sup>2</sup>Departament de Biologia Marina i Oceanografia**  
21 **Institut de Ciències del Mar, CSIC**  
22 **Pg. Marítim de la Barceloneta, 37-49**  
23 **08003 Barcelona, Catalonia, Spain**

24  
25  
26  
27  
28  
29  

---

\* To whom correspondence should be addressed  
Tele: +44 121 414 3494; Fax: +44 121 414 3708; Email: r.m.harrison@bham.ac.uk

† Also at: Department of Environmental Sciences / Center of Excellence in Environmental Studies, King Abdulaziz University, PO Box 80203, Jeddah, 21589, Saudi Arabia

30 **HIGHLIGHTS**

31

32 • Brake wear particles are an important constituent of urban aerosol

33 • ATOFMS identifies brake dust from Fe and Ba signals

34 • High laser pulse energies are needed to detect the Ba<sup>+</sup> ion

35 • Data from several field campaigns are presented

36 **ABSTRACT**

37 Brake dust particles were characterised using an Aerosol Time-of-Flight Mass  
38 Spectrometer (ATOFMS) operated using two inlet configurations, namely the aerodynamic  
39 lens (AFL) inlet and countersunk nozzle inlet. Laboratory studies show that dust particles  
40 are characterised by mass spectra containing ions deriving from Fe and Ba and although  
41 highly correlated to each other, the Fe and Ba signals were mostly detected using the  
42 nozzle inlet with relatively high laser desorption energies. When using the AFL, only [ $^{56}\text{Fe}$ ]  
43 and [ $^{88}\text{FeO}_2$ ] ions were observed in brake dust spectra generated using lower laser  
44 desorption pulse energies, and only above 0.75 mJ was the [ $^{138}\text{Ba}$ ] ion detected. When  
45 used with the preferred nozzle inlet configuration, the [ $^{88}\text{FeO}_2$ ] peak was considered to be  
46 the more reliable tracer peak, because it is not present in other types of dust (mineral, tyre,  
47 Saharan etc). As shown by the comparison with ambient data from a number of locations,  
48 the aerodynamic lens is not as efficient in detecting brake wear particles, with less than  
49 1% of sampled particles attributed to brake wear. Five field campaigns within Birmingham  
50 (background, roadside (3) and road tunnel) used the nozzle inlet and showed that dust  
51 particles (crustal and road) accounted for between 3.1 and 65.9 % of the particles  
52 detected, with the remaining particles being made up from varying percentages of other  
53 constituents.

54

55 **Keywords:** ATOFMS; single particles; traffic emissions; resuspension; brake dust

56

57 **1. INTRODUCTION**

58 Both exhaust and non-exhaust emissions are now the focus of air quality research as  
59 tightening policies are reducing the contribution of engine exhaust to the total airborne  
60 particulate matter budget, such that non-exhaust emissions are becoming more prominent  
61 (Lenschow et al., 2001; Harrison et al., 2001; Querol et al., 2004; Boulter et al., 2006). It is  
62 recognised that road traffic is frequently a dominant, but mitigatable, source of particulate  
63 matter (PM) accounting for 5-80% of airborne concentrations of PM depending on site and  
64 location (Pant and Harrison, 2013). In the UK, the Air Quality Expert Group identified non-  
65 exhaust primary PM emissions from road transport as a priority area of uncertainty, and  
66 stated the need to update and refine the associated methodologies and estimates (AQEG,  
67 2005). Other, international assessments have also highlighted the need for action (Denier  
68 van der Gon et al., 2013; Amato et al., 2014)

69  
70 Non-exhaust emissions arise from mechanical abrasion and corrosion processes leading  
71 to particles with a large proportion in the coarse size range. The most important direct  
72 emission sources are associated with the wear of tyres, brakes, clutch and road surfaces  
73 through abrasion, and vehicle bodywork through corrosion. Compared to tail-pipe  
74 emissions, the coarser nature of non-exhaust emissions implies that they are more likely to  
75 be deposited onto the road surface and then be resuspended into the atmosphere both  
76 due to vehicle-generated turbulence and by action of the wind (Harrison et al., 2001). The  
77 common assumption that most of the primary fine particles ( $PM_{2.5}$ ) and the coarse  
78 particles ( $PM_{2.5-10}$ ) arise from exhaust and non-exhaust emissions respectively is not well  
79 supported by measurement of non-exhaust PM. There is evidence showing that non-  
80 exhaust particles contribute to both the fine and the coarse mode (AQEG 2005) implying a  
81 need for measurement of both size fractions.

82

83 The frictional contact between a brake pad/shoe and disc/drum rotating with the wheel of  
84 the vehicle converts the linear motion of the vehicle into thermal energy. Associated with  
85 this process is the gradual wear of the contacting components which in turn liberates brake  
86 dust. The brake disc/drum is generally fabricated from cast iron and the contact material  
87 of the pads/shoes is made from a range of materials (Thorpe and Harrison, 2008). Recent  
88 information on the composition of brake pads used in Europe is available from Hulskotte et  
89 al. (2014). Major element components on average comprised 23% Fe, 11% Cu, 5% Zn,  
90 and 3% Sn as the dominant metals. Non-metal components in the discs were 2-3% Si, 3%  
91 S and 26% carbon. Hulskotte et al. (2014) do not report measurements of Ba, but cite  
92 reported values of 0.07-6.9% from Spain and 12% from Japan. Correlations have been  
93 observed between Cu, Ba, and Fe observed in ambient particulate matter (Birmili et al.,  
94 2006) and with measurements at roadside (Gietl et al., 2010). Furthermore, using the  
95 robust ratio between Fe and Cu found at the kerbsides, a 70% and 30% estimate of the  
96 contribution of brake pads and brake discs (consisting almost entirely of metal with iron  
97 being the dominant element >95%) to total brake wear respectively was made.

98  
99 Using data from roadside and local background locations, Gietl et al. (2010) estimated that  
100 barium comprises 1.1% of brake wear ( $PM_{10}$ ) particles from the traffic fleet as a whole,  
101 allowing its use as a quantitative tracer of brake wear emissions at traffic-influenced sites.  
102 By using real time aerosol data, Dall'Osto et al. (2013) found that Fe and Cu together can  
103 also be used as a tracer of brake wear. Other studies have reported that the abrasion of  
104 brakes produces particles characterised by high concentrations of Cu, Ba, Zn and Fe  
105 (Sanders et al., 2003; Johansson et al., 2008). Iron is often considered to be related to  
106 crustal elements and resuspension of road dust (Sternbeck et al., 2002; Heal et al., 2005;  
107 Lough et al., 2005). However, Harrison et al. (2003) in devising a pragmatic mass closure  
108 method from analyses of particulate matter collected at UK sites, found that the iron

109 concentration within coarse dusts was much greater at roadside sites than at urban  
110 background sites and this was considered indicative of road traffic and most probably the  
111 vehicles themselves as a source. Birmili et al. (2006) confirmed that iron in coarse  
112 particles could be used as a tracer of vehicle-generated particles, whilst calcium is  
113 primarily a tracer of particles from soil, as also concluded by Harrison et al. (2003). Birmili  
114 et al. (2006), compared trace metal concentrations collected at four different measurement  
115 sites representing different degrees of traffic influence. The size-fractionated ambient PM  
116 analyses showed Fe, Ba and Cu correlated closely in the fraction  $1.5 < D_p < 3.0 \mu\text{m}$  in  
117 urban air. This finding supported the concept that most of these particles are not due to  
118 vehicle-induced resuspension but are directly emitted from abrasion processes.

119

120 Mass spectrometry of atmospheric aerosol has recently been established and has quickly  
121 become the most essential and fastest growing area of aerosol research (Laskin et al.,  
122 2012). Currently none of the available mass spectrometry instruments reaches ideality. For  
123 example, the Aerosol Mass Spectrometer (AMS) provides great quantitative information on  
124 limited number of chemical components (Jimenez et al, 2009), but does not analyse any  
125 species which does not volatilise at  $600^\circ\text{C}$  (i.e. Sea salt, dust, Elemental carbon). The  
126 Aerosol Time-of-Flight Mass Spectrometer (ATOFMS) provides information on many more  
127 chemical components (both refractory and non-refractory, size range 200-3000 nm) than  
128 the AMS, but the information is only semi-quantitative (Pratt and Prather 2012). However,  
129 the ATOFMS' unique strength relies in the fact that it can monitor in real time variations in  
130 the single particle composition. Previous studies have indeed focused on the MS of  
131 different types of dust particles (Silva et al., 2000; Sullivan et al., 2007, 2009, Dall'Osto et  
132 al., 2010, 2014).

133



134 This paper extends such work by application of an Aerosol Time-of-Flight Mass  
135 Spectrometer (ATOFMS) to characterisation of brake wear particles in the size range  
136 between 0.3 and 3.0  $\mu\text{m}$ . Mass spectral fingerprints of different dust particles have been  
137 determined and information at a single particle level is presented from both laboratory  
138 studies and from a number of different field studies in very different environments (at  
139 background, roadside and road tunnel sites). The ATOFMS results shown herein provide  
140 information on single dust particles at very high time resolution (minutes), hence allowing  
141 characterisation of the mixing state of brake wear particles, and comparison of their  
142 temporal trends with other dust particle types and meteorological conditions. We first  
143 report the characterization of single particle mass spectra of brake wear aerosol generated  
144 in the laboratory, with specific key  $m/z$  markers. We then report ambient data across a  
145 number of environments, and we discuss the differences encountered. Finally, correlations  
146 between different types of dust and traffic volume data are used to conclude the study.

147

## 148 **2. EXPERIMENTAL**

### 149 **2.1 Instrumentation**

150 This work reports the use of an Aerosol Time-of-Flight Mass Spectrometer (TSI ATOFMS  
151 3800) for the study of brake dust particles. Since its introduction in the late 1990s, the  
152 ATOFMS has given valuable insights into the size and composition of individual airborne  
153 particles (Gard et al., 1997; Pratt and Prather, 2012). In essence, this instrument provides  
154 an aerodynamic diameter and a positive and negative mass spectrum for each particle  
155 ionised by a pulsed UV laser.

156

157 Two different versions of the ATOFMS are commercially available: ATOFMS TSI model  
158 3800-100 and ATOFMS TSI Model 3800. In the ATOFMS TSI model 3800-100, particles  
159 are sampled through an orifice and accelerated through the aerodynamic lens to the sizing

160 region of the instrument (Su et al. 2004). By contrast, the ATOFMS TSI Model 3800  
161 utilizes a nozzle/skimmer interface for the inlet (Gard et al. 1997). In terms of particle  
162 collection efficiency, the aerodynamic lens provides a major improvement toward smaller  
163 particle sizes compared to nozzle/skimmer inlet. Both instruments measure the  
164 aerodynamic diameter of particles sizes between 100 nm and 3  $\mu\text{m}$  by calculating their  
165 time of flight between two orthogonally positioned continuous wave lasers ( $\lambda = 532 \text{ nm}$ ).  
166 However, a number of factors affecting the potential to extract fully quantitative information  
167 on particle size distributions - i.e. the transmission efficiency of the nozzle/skimmers used  
168 to create the particle beam in the instrument's inlet (Dall'Osto et al., 2006) - make the size  
169 responses of the two instruments quite different. Generally speaking, whilst the ATOFMS  
170 equipped with the lens provides mainly particles below 1  $\mu\text{m}$ , the opposite case is found  
171 for the nozzle/skimmer inlet. Following the particle inlet and sizing part of the inlet,  
172 particles are then transmitted, in both TSI models (aerodynamic lens and nozzle/skimmer),  
173 into the mass spectrometry region of the instruments where the light scattered by the  
174 particles is used to trigger a pulsed high-power desorption and ionization laser ( $\lambda = 266$   
175 nm, about 1 mJ per pulse) that desorbs and ionizes the particle in the centre of the ion  
176 source of a bipolar reflectron ToF-MS. Thus, positive and negative ion spectra of a single  
177 particle are obtained.

178

179 Whilst the efficiency of the NI is heavily biased towards the super-micron aerosol (Gard et  
180 al., 1997), the AFL focuses a narrow particle beam for sizes between 100 nm and 3  $\mu\text{m}$   
181 (Su et al., 2004). Figure S1 compares the efficiencies of the two inlet types. Depending on  
182 the scientific objectives, past studies have typically used the AFL system to study ultrafine  
183 and fine anthropogenic emissions (Spencer et al., 2006) and the NI system has been used  
184 to study dust particles (Sullivan et al., 2007, 2009, Moffet et al., 2012). The combination of  
185 AFL and PMT pre-amplifiers increased the detection of particles (Hit Counts) of particles

186 with a diameter below 1.0  $\mu\text{m}$  by a factor of 100. This is can be exemplified by comparing  
187 ambient data collected using the NI and the AFL with the PMT pre-amplifiers. The mode  
188 in the size distribution below 1.0  $\mu\text{m}$  has greater amplitude for the AFL than the NI  
189 ATOFMS (Figure S3). Furthermore, when considering the size distribution of the brake  
190 dust cluster, the mode is not clearly present for the data collected using the NI ATOFMS.

191

192 It is important to note that a limitation of laser desorption/ionization (LDI) single particle  
193 mass spectrometry is that the process is heavily influenced by particle size, morphology  
194 and matrix composition, since these will influence energy transfer from the laser beam to  
195 the particle, vaporization of the particle and ion formation in the vaporization plume (Reilly  
196 et al., 2000; Schoolcraft et al., 2001).

197

198 Analyses of collected data were carried out using YAADA (Allen et al., 2001) run within the  
199 Matlab version 6.1 environment. The ART-2a neural network algorithm (Song et al., 1999)  
200 was used to reduce the complexity of each dataset by clustering particles into groups with  
201 similar mass spectral properties. ART-2a was applied using a learning rate of 0.05,  
202 vigilance factor 0.85 and a total number of 20 iterations. ART-2a generates a large  
203 number of clusters (in excess of 200) starting with those with a large number of particles,  
204 the main clusters, right down to the minor clusters which only have a few particles. The  
205 identity of the clusters is determined from the mass spectra and those from common  
206 sources are merged back together starting with the main clusters. Usually only the first  
207 40-50 clusters are considered because those beyond 50 have too few mass spectra within  
208 them to be significant.

209

210 The data and clusters presented in this study have been collected in both laboratory and  
211 ambient field studies over a period (2001-2014) during which the ATOFMS inlet was

212 updated from using a nozzle (2001-2006), to an aerosol focussing lens inlet (2006-2014).  
213 In the update, the sensitivity of the ATOFMS to the smaller particles was increased by pre-  
214 amplifying the PMT light scattering signals and the analogue to digital converters used to  
215 read the ion signals from the micro channel plates were changed to increase dynamic  
216 range to stopping 'peak clipping'.

## 217

## 218 **2.2 Characterisation of Brake Wear in Laboratory Studies**

### 219 **2.2.1 Brake wear ATOFMS nozzle orifice (NI) inlet laboratory study**

220 In the early work using the nozzle inlet, brake dust ground from a brake pad was sampled  
221 into the ATOFMS. Mass spectra were obtained by placing each dust sample into a flask in  
222 a sonicator to create a suspension of dust particles under filtered lab air flow (Silva et al.,  
223 2000; Schofield, 2004). The aerosol was then directed into the ATOFMS inlet for analysis  
224 and about 1000 single-particle mass spectra were collected per sample. Due to the large  
225 range of brake pads used on vehicles and the limited information on composition, brake  
226 pads used on the ten best selling cars for 2001 in the United Kingdom (SMMT, 2002) were  
227 sampled using this method together with dust accumulated behind the wheel trim of a front  
228 wheel of a car (Schofield, 2004). The same methods have been applied in later studies  
229 (Sullivan et al., 2007, 2009; Dall'Osto et al., 2010).

### 230

### 231 **2.2.1 Brake wear ATOFMS aerodynamic lens (AFL) inlet laboratory study**

232 In later work using the AFL inlet, an automotive brake and calliper system was housed  
233 within a small enclosure. Brake dust was sampled from the enclosure directly by the  
234 ATOFMS. The disc was rotated by an electric motor and compressed air was used to force  
235 the brake pads onto the disc which was rotated at 1500 rpm corresponding to  
236 approximately 111 mph for a typical 65 cm diameter car wheel. Various brake pressures

237 (1-4 bar) were then applied which corresponded to light, medium and heavy braking  
238 raising the temperature of the back surface of the brake pad to over 60°C.

239

## 240 **2.3 Field Studies**

### 241 **2.3.1 Ambient field study using the nozzle inlet (NI)**

242 During June and July 2002 the ATOFMS was deployed in Birmingham (UK). The aim of  
243 this work was to compare the composition of particles collected at each of three  
244 contrasting sites and to assess the application of the ATOFMS in source apportionment.  
245 Three different sites were chosen, each of which had differing degrees of traffic influence:

246 (i) The *Winterbourne* (WB) site, was an urban background site on the east side of the  
247 University of Birmingham campus (52°27'13"N; 01°55' 27"W). The location is within a  
248 residential area with the nearest road 100 m to the west and the busy A38 road, 500  
249 m to the South. This urban background site was expected to be representative of the  
250 urban background PM on a scale of several km.

251 (ii) The *Queensway Underpass* (QW) site is part of the tunnel network that carries traffic  
252 to and from the M6 motorway under central Birmingham (52°28'47"N; 01°54'21"W).  
253 The tunnel is approximately 200 m long with the north-bound and south-bound lanes  
254 separated by a wall, with occasional gaps. The sampling site within the tunnel was in  
255 an emergency lay-by recessed into the walls of the bore for south-bound traffic. On  
256 travelling through the tunnel traffic is limited to 30 mph and has to take a left hand  
257 turn passing the sampling site before exiting the tunnel.

258 (iii) The *Bristol Road* (BR) site, is within the grounds of the University of Birmingham  
259 overlooking the busy A38 which is a major highway that runs from south-west to  
260 north-east through Birmingham (52°26'50"N; 01°55'42 "W). The traffic speed is again  
261 limited to 30 mph and the observatory was placed within 50 m of a traffic light  
262 controlled junction. The traffic volume at the roadside site was 22,000 vehicles per

263 day, with about 7% being heavy duty trucks and buses. Three campaigns were  
264 conducted at this site.

265

266 The ATOFMS was deployed in the three different locations for a total period of 17 days.  
267 Detailed information on starting time, sampling duration and total number of particles  
268 detected are given in Table 1.

269

### 270 **2.3.2 Ambient field study using the aerodynamic lens (AFL) inlet**

271 Following an upgrade in 2006, the NI inlet was replaced by the AFL system after which 3  
272 subsequent field studies that were carried out at the following sites in London, Port Talbot  
273 and Barcelona:

274 (i) The *Marylebone Road (MR) site* is located on kerbside of a major arterial route within  
275 the city of Westminster in London (51°31'21"N; 00°09'17"W). This is on a heavily  
276 trafficked (ca. 80,000 vpd) six lane highway running through a street canyon in  
277 central London.

278 (ii) The *Port Talbot (PT) site* is located in the grounds of Margam Fire Station in South  
279 Wales located in South Wales (51°35'03"N; 03°46'16" W) 250 m away from the M4  
280 motorway (ca 50,000 vpd). Port Talbot is a coastal industrial town with a population  
281 of approximately 35,000 and the Tata steelworks is the main industry area covering  
282 approximately 28 km<sup>2</sup>, having a production capacity around 5 million tonnes per year.

283 (iii) The *Barcelona (BCN) Road site* (41°23'18"N; 02°09'00"E) was situated in a car park  
284 of the Escuela de Ingeniería Técnica Industria (St. Urgell, 187 – elevation 40 m a.s.l.)  
285 next to C/ Urgell, a major highway composed of a one-way four lane road (17,000  
286 vpd). With a population of about 1.7 million inhabitants in the city and around 4  
287 million in the surrounding area, Barcelona is the fifth most populated metropolitan  
288 area in Europe.





315 [ $^{88}\text{FeO}_2$ ] and [ $^{104}\text{FeO}_3$ ]), barium ([ $^{138}\text{Ba}$ ], [ $^{154}\text{BaO}$ ], [ $^{210}\text{FeBaO}$ ], and [ $^{226}\text{FeBaO}_2$ ]) although  
316 only the more prominent peaks are seen in the average spectra of Figure 1. The negative  
317 ATOFMS mass spectrum is mainly composed of elemental carbon peaks at  $m/z$  [ $^{12}\text{C}$ ], [ $^{36}\text{C}_3$ ], [ $^{48}\text{C}_4$ ], and [ $^{60}\text{C}_5$ ]. It is important to remember that the ATOFMS uses a 266 nm  
318 wavelength for ionisation - and as such maybe biased towards the EC signature (due to  
319 different absorption efficiencies and ionization potentials) - implying the ATOFMS will be  
320 more sensitive to particles containing traces of EC relative to others containing OC.  
321 Furthermore, copper peaks ([Cu],  $m/z$  63 and 65) were seen in about 30% of the particles  
322 analysed and interestingly some of the mass spectra indicated the presence of antimony  
323 and its oxides in both positive and negative spectra ([ $\text{SbO}_2$ ] $^+$ ,  $m/z$  +/- 153 and 155, [ $\text{SbO}_4$ ] $^+$ ,  
324  $m/z$  -185 and -187).

326

327 The positive mass spectrum of brake wear material detected with the AFL inlet (Figure 1b)  
328 was similar to that measured with the NI (Figure 1a), with the exception of the strong  
329 presence of chlorides ([ $^{35}\text{Cl}$ ]), nitrates ([ $^{46}\text{NO}_2$ ] and [ $^{62}\text{NO}_3$ ]), and phosphates ([ $^{63}\text{PO}_2$ ]  
330 and [ $^{79}\text{PO}_3$ ]) in the negative spectra. Barium peaks [Ba] and [BaO] ( $m/z$  138 and 154)  
331 were only observed using the nozzle inlet when comparing lab experiments. This  
332 discrepancy can be explained by a difference in the available laser desorption energy  
333 during the lab experiments and an energy threshold of 0.74 mJ for barium. The NI-  
334 ATOFMS used 0.85 mJ whereas the AFL-ATOFS used 0.19 mJ. Figure S4 plots the  
335 percentage occurrence of [ $^{56}\text{Fe}$ ], [ $^{88}\text{FeO}_2$ ] and [ $^{154}\text{BaO}$ ] in the field data (discussed below)  
336 as a function of laser energy and it is clear that [ $^{138}\text{Ba}$ ] occurs only at higher energies  
337 above 0.74 mJ. This later led us to understand - in the Field Studies section below - why  
338 barium peaks were observed in the MR2009 and not the BCN2010 ambient data sets  
339 (Figure 2). For MR2009 and BCN2010, the laser energies were 0.79 mJ and 0.74 mJ  
340 respectively, above and below the threshold.



341 A dependence of the brake dust tracer peaks ( $[^{56}\text{Fe}]$ ,  $[^{88}\text{FeO}_2]$ ,  $[^{138}\text{Ba}]$  and  $[^{154}\text{BaO}]$  was  
342 also observed as a function of particle diameter (Figure S2). As the aerodynamic diameter  
343 of the brake dust particles increased to, and passed 1  $\mu\text{m}$ , the fraction of  $[^{88}\text{FeO}_2]$  and  
344  $[^{138}\text{Ba}]$  and  $[^{154}\text{BaO}]$  detected increased. Again,  $[^{56}\text{Fe}]$  proves to be the most reliable tracer  
345 peak, being detected in 100% of the particles with aerodynamic diameters between 0.7  
346 and 2.0  $\mu\text{m}$  for both the NI and AFL. As for  $[^{88}\text{FeO}_2]$ , there was between 60% and 80%  
347 occurrence for particles greater than 0.9  $\mu\text{m}$  detected using the NI and AFL. And similarly,  
348 for the  $[^{138}\text{Ba}]$  peak there was a 40% detection for both the NI and AFL, for particles of  
349 diameter greater than  $\sim 0.7$  and  $\sim 1.2$   $\mu\text{m}$  respectively. Thus  $[^{56}\text{Fe}]$  and  $[^{88}\text{FeO}_2]$  are more  
350 reliable markers for brake wear particles than  $[\text{Ba}]$  and  $[\text{BaO}]$  across all particle sizes.  
351 Furthermore, for the NI it was also realised that although soil particle spectra contained  
352  $[^{56}\text{Fe}]$  peaks,  $[^{88}\text{FeO}_2]$  peaks were observed very infrequently. According to Figure S2, at  
353 smaller particle sizes ( $< 1$   $\mu\text{m}$ ) there is a loss in sensitivity to the ions characteristic of brake  
354 dust. This may be due to inhomogeneities in the brake dust particles, which would imply  
355 that the composition may vary within the sub-micrometre size range. The larger particles  
356 contain sufficient material that this effect is “averaged out”.

357

358 In summary, the characteristic features of brake wear particle types include intense  $[^{56}\text{Fe}]$   
359 and  $[^{88}\text{FeO}_2]$  signals, along with  $[^{138}\text{Ba}]$  and  $[^{154}\text{BaO}]$ . However, whilst the Ba marker is  
360 sensitive to the laser fluence, the Fe signals are not. Moreover, it is important to note that  
361 very few  $[^{88}\text{FeO}_2]$  peaks are observed in other types of dust, including soil (Dall’Osto and  
362 Harrison, 2006), Saharan dust (Dall’Osto et al., 2010), Asian mineral dust (Moffet et al.,  
363 2012) and tyre dust (Dall’Osto et al., 2014). This iron cluster  $[^{88}\text{FeO}_2]$ , along with the  
364 strong presence of  $[^{138}\text{Ba}]$  is therefore a good indicator of brake dust particles.

365

366

367 **3.2 Ambient Field Studies of Brake Dust**

368 Five field studies were carried out in Birmingham UK, using the ATOFMS fitted with the  
369 nozzle inlet (Table 1) in which 201,746 mass spectra of particles were measured and  
370 subsequently classified into clusters using ART-2a. A number of mass spectra detected  
371 were similar to those shown in Figure 1a and apportioned to brake dust. The average  
372 brake dust mass spectrum detected in the Birmingham studies with the NI-ATOFMS is  
373 shown in Fig. 2a, clearly showing specific markers due to iron ( $m/z$  56,  $m/z$  -88) and  
374 barium ( $m/z$  138 and  $m/z$  154). Other dust particle types were detected, including  
375 vegetative debris (5.2 % at BR2002 only, Table S1) and road dust (3.1-8.2 % across all 5  
376 campaigns Table S1), but none of these contained the brake wear markers identified in  
377 this study.

378

379 Previous ATOFMS studies with NI-ATOFMS carried out in other locations have also  
380 reported this cluster. Dall'Osto et al. (2006) in Athens, Greece showed a cluster named  
381 'car' - correlating with rush hour traffic - with strong signals at  $m/z$  54, 56 and -88 due to  
382 iron [ $^{54}\text{Fe}$ ], [ $^{56}\text{Fe}$ ] and [ $^{-88}\text{FeO}_2$ ], respectively). Peaks at  $m/z$  138 and 154 are due to barium  
383 ([ $^{138}\text{Ba}$ ] and [ $^{154}\text{BaO}$ ]).

384

385 The average ATOFMS mass spectrum of particles attributed to brake dust collected at two  
386 European sites with the AFL inlet is shown in Figures 2b and c. . The peaks are due to  
387 sodium ([ $^{23}\text{Na}$ ]), aluminium ([ $^{27}\text{Al}$ ]), potassium ([ $^{39}\text{K}$ ]), iron ([ $^{56}\text{Fe}$ ], [ $^{\pm 72}\text{FeO}$ ], [ $^{112}\text{Fe}_2$ ],  
388 [ $^{128}\text{Fe}_2\text{O}$ ], [ $^{-88}\text{FeO}_2$ ] and [ $^{-104}\text{FeO}_3$ ]), barium ([ $^{138}\text{Ba}$ ], [ $^{154}\text{BaO}$ ], [ $^{210}\text{FeBaO}$ ], and  
389 [ $^{226}\text{FeBaO}_2$ ]), chlorides ([ $^{-35}\text{Cl}$ ]), nitrates ([ $^{-46}\text{NO}_2$ ] and [ $^{-62}\text{NO}_3$ ]), and phosphates ([ $^{-63}\text{PO}_2$ ])  
390 and ([ $^{-79}\text{PO}_3$ ]). These show similar tracer peaks of Fe,  $\text{FeO}_2^-$  and Ba although these are  
391 less frequently observed as the LDI laser energy decreased towards the Ba-LDI threshold.

392

393 Following the modification of the ATOFMS to use the AFL, brake wear particles were  
394 detected less often in urban field studies, and in some comparisons were not detected at  
395 all at background sites (Smith et al., 2012; Dall'Osto et al., 2009). Consequently we have a  
396 relatively low percentage of brake wear particles detected at MR2009 (1.0%), BCN2010  
397 (0.3%) and PT2012 (~10%). Fe-rich particles associated with brake wear were detected at  
398 Marylebone Road (Figure 2) although Giorio et al. (2015) did not identify any Fe-rich  
399 particles in this Marylebone Road data set using the *k*-Means method. The clusters used  
400 in that study only accounted for 55% of the variance and when the spectral data base was  
401 queried, 1.5% of the dataset were identified as Fe-rich. Of these, 17% were attributed to  
402 brake wear, with spectra similar to those measured in the laboratory studies shown in  
403 Figure 1.

404

405 In the road dust samples, brake wear material was found only on the Marylebone Road  
406 and at very low percentages (2%). This is similar to the observation by Dall'Osto et al.  
407 (2014) which showed that tyre dust is a minor component of road dust, but unlike brake  
408 dust, tyre dust is internally mixed with the road dust as a result of the high adhesion forces  
409 resulting from the surface properties of the tyre rubber.

410

#### 411 **4. DISCUSSION**

412 This study considers roadside and laboratory studies of brake dust emissions measured  
413 using an Aerosol Time-of-Flight Mass Spectrometer (TSI 3800 - ATOFMS). The results  
414 presented using the two possible inlet configurations (aerodynamic lens and nozzle inlet)  
415 show that brake dust particles are characterised by ion peaks at  $m/z$  [ $^{56}\text{FeO}_2$ ] and [ $^{138}\text{Ba}$ ]  
416 and have a size distribution with a modal diameter in the ATOFMS data of 1.5  $\mu\text{m}$   
417 aerodynamic diameter corresponding to an actual modal diameter of 1.3  $\mu\text{m}$  after  
418 correction for inlet efficiency.

419

420 Table 1 includes a summary of the brake dust percentages detected at three urban sites in  
421 Birmingham UK during five different seasons spread over three years. The highest relative  
422 concentration of dust detected was at the tunnel site (QW2002), of which 60% of the total  
423 dust particles analysed were categorised as brake dust with the remaining dust particles  
424 being classified as road dust.

425

426 To our knowledge there are only a few studies which have reported brake wear material in  
427 urban environment at high time resolution. These includes ATOFMS studies (Gross et al.,  
428 2000; Dall'Osto and Harrison, 2006), and a recent PIXE paper (Dall'Osto et al., 2013)  
429 where a Fe-Cu particle type was reported at hourly time resolution. However, not only high  
430 time resolution but also high number counts are needed in order to draw meaningful  
431 conclusions on brake wear particles. The Queensway tunnel experiment gave us very high  
432 time resolution, but also a very high number of brake wear material particles. Indeed  
433 Figure 3a shows the temporal trend of these two types of dust (Brake and Road dust)  
434 detected at the tunnel site. There is a close, but not exact temporal correlation between  
435 both road dust and brake dust and the hourly vehicle count (Figure 3(a)). The slight  
436 differences between the times of the peaks may have arisen for a number of reasons.  
437 Traffic counts were taken for only 15 minutes of each hour and may not fully represent the  
438 entire hour. Also, there is no certainty of a constancy of the ventilation conditions of the  
439 tunnel, which along with source strength determine airborne concentrations. The vehicle  
440 fleet mix and driving mode may also have changed during the course of the day, thus  
441 influencing emissions. In comparison, at the roadside site, road dust correlated with  
442 Vegetative/Soil Dust ( $r = 0.65$ ) (Figure 3b) and brake dust deviated from the trend showing  
443 a tendency to peak during the rush hour periods). The observation that brake dust  
444 particles are detected as a separate cluster to resuspended road dust, suggests that brake

445 dust is emitted directly into the atmosphere to be dispersed, with only a small amount  
446 settling into road dust. Alternatively, some may deposit to the road surface, but not be  
447 effectively resuspended.

448

449 Lough et al. (2005) reported that iron was the most abundant element in  $PM_{10}$  emitted in a  
450 road tunnel, and it was attributed mainly to brake wear emissions and resuspension of  
451 road dust. The size-resolved data for Fe presented correlate more closely with brake wear  
452 elements (Ba, Cu, Sb) rather than with crustal elements (Mg, Ca) which exhibit a coarser  
453 mode. Iron dominated the contribution of trace metals to total metal mass in all particle  
454 fractions ( $PM_{2.5}$ ,  $PM_{2.5-10}$  and  $PM_{10}$ ) in a study conducted at Edinburgh (UK) (Heal et al.,  
455 2005). Both Birmili et al. (2006) and Harrison et al. (2003) reported that coarse Fe can be  
456 used as a tracer of vehicle-generated material. There are clearly important differences in  
457 the amount of Fe-related particles which arise from vehicle-induced resuspension and  
458 from the direct emission of abrasion products respectively

459

460 Aerosol emissions in road tunnels have been reported from several studies conducted in  
461 different locations. Sternbeck et al. (2002) reported that Cu, Zn, Cd, Sb, Ba and Pb were  
462 the most strongly enriched metals for which direct vehicle emissions are much more  
463 important than resuspension for their presence in the aerosol. On the other hand, Al, Ca,  
464 Ce, Fe, Mg, Mn and Ti were attributed to the resuspension of dust in the tunnels. However,  
465 it is important to note that the metal data reported by Sternbeck et al. (2002) were from the  
466 total particulate matter fraction. On the other hand, Gillies et al. (2001) reported that in the  
467  $PM_{10}$  size fraction, the third most prominent species was iron, and apportioned a  
468 significantly greater mass to geological material, indicative of a substantial contribution  
469 from resuspended dust.

470

471 The mass spectral properties of other dust types (see Figure S5) serve to distinguish them  
472 clearly from the brake wear particles. In the Queensway tunnel (QW2002 site), most of  
473 the dust particles in the measured size range were due to brake dust and only a minor  
474 proportion to road dust. Sampling of particles from road surfaces in London for analysis by  
475 ATOFMS failed to detect particles characteristic of brake wear. Although measured in the  
476 ambient air, the brake dust cluster was not measured in dust samples swept from Regents  
477 Park, or a minor road (near the BT tower within the congestion zone). In fact, the cluster  
478 was only detected as 2% of the mass spectra generated from road dust samples swept  
479 from Marylebone Road. These particles are likely to be emitted by vehicles but it seems  
480 only a small percentage is deposited on the road and resuspended.

481

482 Birmili et al. (2006) found that in the same Queensway road tunnel, PM concentrations (<  
483 0.5  $\mu\text{m}$ ) were enriched by a factor of 7.5, PM (1.5-3.0  $\mu\text{m}$ ) by a factor of 5.3 and PM (3.0-  
484 7.2  $\mu\text{m}$ ) by a factor of 2.6 compared to average urban background levels. The additional  
485 material is expected to originate from direct vehicle emissions.

486

487 Furthermore, time series collected in real time and in-situ show no association of brake  
488 wear particles with road dust and lead to the conclusion that the main proportion of brake  
489 dust in the PM<sub>2.5</sub> fraction is suspended directly from the braking system and dispersed in  
490 the atmosphere, with only a minor amount deposited on the road and resuspended. No  
491 conclusion can be drawn for the PM<sub>10</sub> fraction, in which resuspension of Fe-rich dust  
492 particles is more likely to play an important role.

493

494 Regarding the other urban sites, the background site showed the smallest percentage of  
495 road dust particles, with only 3.1% of the particles sampled being of this type, and  
496 surprisingly no brake dust particles. At the roadside site, a lower proportion of dust

497 particles were detected during wintertime (BR2003; 8.7%; Table S1) than in the two field  
498 studies conducted during the warmer months (BR2002 and BR2004, 25.2% and 20.3%,  
499 respectively; Table S1). This is likely to be due to wet conditions during wintertime.

500

## 501 **5. CONCLUSIONS**

502 In earlier work (Dall'Osto et al., 2014) we have shown the power of the ATOFMS to identify  
503 tyre dust particles in the atmosphere. This latest work characterises in detail the capability  
504 of the ATOFMS to identify brake wear particles which inevitably include particles deriving  
505 both from the brake pad/shoe and disc/drum. The most frequently observed characteristic  
506 peaks in the ATOFMS mass-spectra of brake wear particles are [<sup>56</sup>Fe] and [<sup>88</sup>FeO<sub>2</sub>]. The  
507 former peak is also frequently associated with other sources of iron such as soil dust but  
508 the latter peak appears to be highly characteristic of brake wear. However, the presence  
509 of peaks due to [<sup>138</sup>Ba] and [<sup>154</sup>BaO] is the strongest indicator for brake wear particles as  
510 there few other sources of barium in the atmosphere but these appeared in the mass  
511 spectra only at higher laser energies and it is recommended that individual instruments are  
512 tested with brake wear samples to establish whether such peaks are visible at the laser  
513 energies used. We show that we can separate brake wear dust from other types of dust,  
514 mainly using the peak at m/z -88. This peak is not seen in steel industry (Dall'Osto et al.,  
515 2008) Asian (Sullivan et al., 2007; Moffett et al., 2012) or Saharan dust (Dall'Osto et al.,  
516 2010).

517

518 Full quantification of brake wear particles in the atmosphere has not been attempted as  
519 part of this study and would require a detailed characterisation of instrumental efficiencies  
520 (inlet and ionisation) which was beyond the scope of the current work. Confirmation of the  
521 use of barium as a marker element for brake wear particles supports the approach used by  
522 Gietl et al. (2010) of estimating brake wear particle concentrations from airborne

523 concentrations of this element. It should, however, be noted that brake wear composition  
524 varies from country to country and is subject to change with time. Consequently any  
525 method applied to the quantification of brake dust particles in the atmosphere including the  
526 ATOFMS would need to be calibrated against local conditions before the data were used  
527 for quantification purposes. Nevertheless, we show that brake wear particles generated in  
528 the laboratory and in the ambient air are very similar (contrary to tyre dust which interacts  
529 with road surface material). In addition, we see that brake wear is a source of iron that is  
530 likely to be from a different iron source to dust road and other mineral dust.

531

### 532 **ACKNOWLEDGEMENTS**

533 This work was supported by the UK National Centre for Atmospheric Science.

534



## REFERENCES

- 535  
536  
537 Allen, J.O. et al., 2001 YAADA (Yet Another ATOFMS Data Analyzer) Software Toolkit to  
538 Analyze Single-Particle Mass Spectral Data <http://www.yaada.org/>  
539
- 540 Amato, F., Alastuey, A., de la Rosa, J., Gonzalez Castanedo, Y., Sánchez de la Campa,  
541 A. M., Pandolfi, M., Lozano, A., Contreras González, J., Querol, X., 2014. Trends of road  
542 dust emissions contributions on ambient air particulate levels at rural, urban and industrial  
543 sites in southern Spain. *Atmospheric Chemistry & Physics* 14, 3533–3544.  
544
- 545 AQEG, 2005. Particulate matter in the United Kingdom. Report of the UK Air Quality  
546 Expert Group. Prepared at the request of the Department for Environment Food and Rural  
547 Affairs, London, PB10580 ISBN 0-85521-143-1.  
548
- 549 Birmili, W., Allen, A.G., Bary, F., Harrison, R.M., 2006. Trace metal concentration and  
550 water solubility in size-fractionated atmospheric particles and influence of road traffic.  
551 *Environment Science & Technology* 40, 1144-1153.  
552
- 553 Boulter, P.G., Wayman, M., McCrae, I.S., and Harrison, R.M., 2006. A Review of  
554 Abatement Measures for Non-Exhaust Particulate Matter from Road Vehicles, Published  
555 Project Report PPR230, CPEA23, TRL Limited. [http://uk-  
556 air.defra.gov.uk/assets/documents/reports/cat15/0706061643\\_Report4\\_Abatement\\_meas-  
557 ures.pdf](http://uk-air.defra.gov.uk/assets/documents/reports/cat15/0706061643_Report4_Abatement_measures.pdf)  
558
- 559 Dall'Osto, M., Harrison, R.M., 2006. Chemical characterisation of single airborne particles  
560 in Athens (Greece) by ATOFMS. *Atmospheric Environment* 40, 7614-7631.  
561
- 562 Dall'Osto, M., Harrison, R.M., Beddows, D.C.S., Freney, E.J., Heal, M.R., Donovan, R.J.,  
563 2006. Single particle detection efficiencies of aerosol time-of-flight mass spectrometry  
564 during the North Atlantic marine boundary layer experiment. *Environmental Science &  
565 Technology* 40, 5029-5035.  
566
- 567 Dall'Osto, M., Booth, M.J., Smith, W., Fisher, R., Harrison, R.M., 2008. A study of the size  
568 distributions and the chemical characterisation of airborne particles in the vicinity of a large  
569 integrated steelworks. *Aerosol Science & Technology* 42, 981-991.  
570
- 571 Dall'Osto, M., Harrison, R.M., Coe, H., Williams, P.I., Allan, J.D., 2009. Real time chemical  
572 characterization of local and regional nitrate aerosols. *Atmospheric Chemistry and Physics*  
573 9, 3709-3720.  
574
- 575 Dall'Osto, M., Harrison, R.M., Highwood, E.J., O'Dowd, C., Ceburnis, D., Querol, X.,  
576 Achterberg, E.P., 2010. Variation of the mixing state of Saharan dust particles with  
577 atmospheric transport. *Atmospheric Environment* 44, 3135-3146.  
578
- 579 Dall'Osto, M., Querol, X., Amato, F., Karanasiou, A., Lucarelli, F., Nava, S., Calzolari, G.,  
580 and Chiari, M., 2013. Hourly elemental concentrations in PM<sub>2.5</sub> aerosols sampled  
581 simultaneously at urban background and road site during SAPUSS – diurnal variations and  
582 PMF receptor modelling. *Atmospheric Chemistry & Physics* 13, 4375-4392.  
583
- 584 Dall'Osto, M., Beddows, D.C.S., Gietl, J.K., Olatunbosun, O.A., Yang, X., Harrison, R.M.,  
585 2014. Characteristics of Tyre Dust in Polluted Air: Studies by Single Particle Mass  
586 Spectrometry (ATOFMS). *Atmospheric Environment* 94, 224-230.

- 587 Denier van der Gon, H.A.C., Gerlofs-Nijland, M.E., Gehrig, R., Gustafsson, M., Janssen,  
588 N., Harrison, R.M., Hulskotte, J., Johansson, C., Jozwicka, M., Keuken, M., Krijgsheld, K.,  
589 Ntziachristos, L., Riediker, M., Cassee, F.R., 2013. The Policy Relevance Of Wear  
590 Emissions From Road Transport, Now And In The Future – An international workshop  
591 report and consensus statement. *Journal of the Air & Waste Management Association* 63,  
592 136-149.  
593
- 594 Gard, E., Mayer, J.E., Morrical, B.D., Dienes, T., Fergenson, D.P., Prather, K.A., 1997.  
595 Real-time analysis of individual atmospheric aerosol particles: Design and performance of  
596 a portable ATOFMS. *Analytical Chemistry* 69, 4083-4091.  
597
- 598 Gietl, J.K., Lawrence, R., Thorpe, A.J., Harrison, R.M., 2010. Identification of brake wear  
599 particles and derivation of a quantitative tracer for brake dust at a major road.  
600 *Atmospheric Environment* 44 141-146.  
601
- 602 Gillies, J.A., Gertler, A.W., Sagebiel, J.C., Dippel, L.W.A., 2001. On-road particulate  
603 matter (PM<sub>2.5</sub> and PM<sub>10</sub>) emissions in the Sepulveda Tunnel, Los Angeles, California.  
604 *Environmental Science & Technology* 35, 1054-1063.  
605
- 606 Giorio, C., Tapparo, A., Dall'Osto, M., Beddows, D.C., Esser-Gietl, J.K., Healy, R.M.,  
607 Harrison, R.M., 2015. Local and regional components of aerosol in a heavily trafficked  
608 street canyon in central London derived from PMF and cluster analysis of single-particle  
609 ATOFMS spectra. *Environmental Science & Technology* 49, 3330-3340.  
610
- 611 Giorio, C., Tapparo, A., Dall'Osto, M., Harrison, R.M., Beddows, D.C.S., DiMarco, C.,  
612 Nemitz, E., 2012. Comparison of three techniques for analysis of data from an Aerosol  
613 Time-of-Flight Mass Spectrometer. *Atmospheric Environment* 61, 316-326.  
614
- 615 Gross, D.S., Galli, M.E., Silva, P.J., Wood, S.H., Liu, D.Y., Prather, K.A., 2000. Single  
616 particle characterization of automobile and diesel truck emissions in the Caldecott Tunnel.  
617 *Aerosol Science and Technology* 32, 152-163.  
618
- 619 Harrison, R.M., Yin, J., Mark, D., Stedman, J., Appleby, R.S., Booker, J., Moorcroft S.,  
620 2001. Studies of the coarse particle (2.5-10  $\mu\text{m}$ ) component in UK urban atmospheres.  
621 *Atmospheric Environment* 35, 3667-3679.  
622
- 623 Harrison, R.M., Jones, A.M., Lawrence R.G., 2003. A pragmatic mass closure model for  
624 airborne particulate matter at urban background and roadside sites. *Atmospheric*  
625 *Environment* 37, 4927-4933.  
626
- 627 Heal, M.R., Hibbs, L.R., Agius, R.M., Beverland, I.J., 2005. Total and water-soluble trace  
628 metal content of urban background PM<sub>10</sub>, PM<sub>2.5</sub> and black smoke in Edinburgh, UK.  
629 *Atmospheric Environment* 39, 1417-1430.  
630
- 631 Hopke, P.K., Lamb, R.E., Matusch, D.F.S., 1980. Multielemental characterization of urban  
632 roadway dust. *Environmental Science & Technology* 14, 164-172.  
633
- 634 Hulskotte, J.H.J., Roskam, G.D., Denier van der Gon H.A.C., 2014. Elemental  
635 composition of current automotive braking materials and derived air emission factors.  
636 *Atmospheric Environment* 99 436-445.  
637

- 638 Jimenez, J.L., Canagaratna, M.R., Donahue, N.M., Prevot, A.S.H., Zhang, Q., Kroll, J.H.,  
639 DeCarlo, P.F., Allan, J.D., Coe, H., Ng, N.L., Aiken, A.C., Docherty, K.S., Ulbrich, I.M.,  
640 Grieshop, A.P., Robinson, A.L., Duplissy, J., Smith, J.D., Wilson, K.R., Lanz, V.A., Hueglin,  
641 C., Sun, Y.L., Tian, J., Laaksonen, A., Raatikainen, T., Rautiainen, J., Vaattovaara, P.,  
642 Ehn, M., Kulmala, M., Tomlinson, J.M., Collins, D.R., Cubison, M.J., Dunlea, E.J.,  
643 Huffman, J.A., Onasch, Alfarra, M.R., Williams, P.I., Bower, K., Kondo, Y., Schneider, J.,  
644 Drewnick, F., Borrmann, S., Weimer, S., Demerjian, K., Salcedo, D., Cottrell, L., Griffin, R.,  
645 Takami, A., Miyoshi, T., Hatakeyama, S., Shimono, A., Sun, J.Y., Zhang, Y.M., Dzepina, K.,  
646 Kimmel, J.R., Sueper, D., Jayne, J.T., Herndon, S.C., Trimborn, A.M., Williams, L.R.,  
647 Wood, E.C., Middlebrook, A.M., Kolb, C.E., Baltensperger, U., Worsnop, D.R., 2009.  
648 Evolution of organic aerosols in the atmosphere. *Science*, 326, 1525-1529.  
649
- 650 Johansson, Ch., Norman, M., Burman, L., 2008. Road traffic emission factors for heavy  
651 metals. *Atmospheric Environment* 43, 4681-4688.  
652
- 653 Laskin, A., Laskin, J., Nizkorodov, S.A., 2012. Mass spectrometric approaches for  
654 chemical characterisation of atmospheric aerosols: critical review of the most recent  
655 advances. *Environmental Chemistry* 9, 163-189.  
656
- 657 Lenschow, P., Abraham, H.J., Kutzner, K., Lutz, M., Preu, J.D., Reichenbacher, W., 2001.  
658 Some ideas about the sources of PM<sub>10</sub>. *Atmospheric Environment* 35, 23-33.  
659
- 660 Lough, G.C., Schauer, J.J., Park, J.-S., Shafter, M.M., Deminter, J.T., Weinstein, J.P.,  
661 2005. Emissions of metals associated with motor vehicle roadways. *Environmental*  
662 *Science and Technology* 39, 826-836.  
663
- 664 Moffet, R.C., Furutani, H., Rödel, T.C., Henn, T.R., Sprau, P.O., Laskin, A., Uematsu, M.,  
665 Gilles, M.K., 2012. Iron speciation and mixing in single aerosol particles from the Asian  
666 continental outflow. *Journal of Geophysical Research* 117, D07204,  
667 doi:10.1029/2011JD016746,  
668
- 669 Pant, P., Harrison, R.M. 2013. Estimation of the contribution of road traffic emissions to  
670 particulate matter concentrations from field measurements: A review. *Atmospheric*  
671 *Environment* 77, 78-97.  
672
- 673 Pratt, K.A., Prather, K., 2012. Mass spectrometry of atmospheric aerosols – Recent  
674 developments and applications. Part II: On-line mass spectrometry techniques. *Mass*  
675 *Spectrometry Reviews* 31, 17-48.  
676
- 677 Querol, X., Alastuey, A., Ruiz, C.R., Artinano, B., Hansson, H.C., Harrison, R.M., Buringh,  
678 E., ten Brink, H.M., Lutz, M., Brüchmann, P., 2004. Speciation and origin of PM<sub>10</sub> and  
679 PM<sub>2.5</sub> in selected European cities. *Atmospheric Environment* 38, 6547-6555.  
680
- 681 Reilly, P.T.A., Lazar, A.C., Gieray, R.A., Whitten, W.B., Ramsey, J.M., 2000. The  
682 elucidation of charge-transfer-induced matrix effects in environmental aerosols via real-  
683 time aerosol mass spectral analysis of individual airborne particles. *Aerosol Science &*  
684 *Technology* 33, 135-152.  
685
- 686 Sanders, P.G., Xu, N., Dalka, T.M., Maricq, M.M., 2003. Airborne brake wear debris: Size  
687 distributions, composition, and a comparison of dynamometer and vehicle tests.  
688 *Environmental Science & Technology* 37, 4060-4069.  
689

- 690 Schofield, M.J., 2004. Sources and properties of airborne particulate matter. Ph.D. Thesis,  
691 School of Geography, Earth and Environmental Sciences, University of Birmingham.  
692
- 693 Schoolcraft, T.A., Constable, G.S., Jackson, B., Zhigilei, L.V., Garrison, B.J., 2001.  
694 Molecular dynamics simulations of laser disintegration of amorphous aerosol particles with  
695 spatially non- uniform absorption. Nuclear Instruments and Methods in Physics Research  
696 Section B 180, 245-250.  
697
- 698 Silva, P.J., Carlin, R.A., Prather, K.A., 2000. Single particle analysis of suspended soil  
699 dust from Southern California. Atmospheric Environment 34, 1811-1820.  
700
- 701 Smith, S., Ward, M., Lin, R., Brydson, R., Dall'Osto, M., Harrison, R.M., 2012.  
702 Comparative study of single particle characterisation by transmission electron microscopy  
703 and time-of-flight aerosol mass spectrometry in the London atmosphere. Atmospheric  
704 Environment 62, 400-407.  
705
- 706 SMMT, 2002. Motor Industry Facts - 2002. The Motor Industry SMMT.  
707
- 708 Song, X.H., P.K. Hopke, D.P. Fergenson, and K.A. Prather, 1999. Classification of single  
709 particles analyzed by ATOFMS using an artificial neural network, ART-2A. Analytical  
710 Chemistry 71, 860-865.  
711
- 712 Spencer, M.T., Shields, L.G., Sodeman, D.A., Toner, S.M., Prather K.A., 2006.  
713 Comparison of oil and fuel particle chemical signatures with particle emissions from heavy  
714 and light duty vehicles. Atmospheric Environment 40, 5224-5235.  
715
- 716 Sternbeck, J., Sjódin, A., Andreasson, K., 2002. Metal emissions from road traffic and the  
717 influence of resuspension — results from two tunnel studies. Atmospheric Environment  
718 36, 4735-4744.  
719
- 720 Su, Y.X., Sipin, M.F., Furutani, H., Prather, K.A., 2004. Development and characterization  
721 of an aerosol time-of-flight mass spectrometer with increased detection efficiency.  
722 Analytical Chemistry 76, 712-719.  
723
- 724 Sullivan, R.C., Guazzotti, S.A., Sodeman, D.A., Prather, K.A., 2007. Direct observations  
725 of the atmospheric processing of Asian mineral dust. Atmospheric Chemistry & Physics 7,  
726 1213-1236.  
727
- 728 Sullivan, R.C., Moore, M.J.K., Petters, M.D., Kreidenweis, S.M., Roberts, G.C., Prather,  
729 K.A., 2009. Effect of chemical mixing state on the hygroscopicity and cloud nucleation  
730 properties of calcium mineral dust particles. Atmospheric Chemistry & Physics 9, 3303-  
731 3316.  
732
- 733 Thorpe, A., Harrison, R.M., 2008. Sources and properties of non-exhaust particulate matter  
734 from road traffic: A review. Science of the Total Environment 400, 270-282.  
735

## TABLE LEGEND

**Table1:** ATOFMS field studies conducted using the Aerodynamic Focussing Lens (AFL) and Nozzle Inlet (NI).

## FIGURE LEGENDS

**Figure 1:** Average mass spectra of laboratory brake dust particle clusters derived from ART2a using the nozzle inlet and 0.85 mJ laser energy (*left panels*) and AFL inlet and 0.19 mJ laser energy (*right panels*). The top graphs show ion current expressed as an absolute area of the peak. The lower graphs show the fraction of particles having the specified m/z peak.

**Figure 2:** Average mass spectra of ambient brake dust particle clusters derived from ART2a using the nozzle inlet (*left panels* and 0.82 mJ laser energy *BHAM2002*) and AFL inlet (middle panels and 0.79 mJ laser energy *MR2009* and *right panels* 0.74 mJ *BCN2010*). The upper and lower panels are generated as in Figure 1 and *BHAM2002* represents the average of *BR2002* and *QW2002*.

**Figure 3:** (a) Temporal trend of unscaled ATOFMS counts for brake dust and road dust along with number of vehicles detected during the Tunnel experiment (hourly resolution); (b) Time series of three dust types.

**Table 1:** ATOFMS field studies conducted using the Aerodynamic Focussing Lens (AFL) and Nozzle Inlet (NI).

	Nozzle ATOFMS					Aerodynamic lens ATOFMS			
<i>Campaign</i>	<i>WB2002</i>	<i>BR2002</i>	<i>BR2003</i>	<i>BR2004</i>	<i>QW2002</i>	<i>MR2009</i>	<i>BCN2010</i>	<i>PT2012</i>	
<i>Site Type</i>	background	roadside	roadside	roadside	tunnel	roadside	roadside	Industrial	
<i>Period</i>	25- 28/06/2002	08- 12/07/2002	09- 15/12/2003	25- 29/05/2004	02/07/2002 05:00-20:00	22-05-2009 11-06-2009	16-09-2010 16-10-2010	18-04-2012 16-05-2012	
<i>Laser DI Energy (mJ)</i>	-----		0.82	-----		0.79	0.74	0.49	
<i>N°. of mass spectra (per day)</i>	18,359 (6,120)	35,763 (8,941)	67,943 (1,132)	68,709 (17,177)	10,972 (17,555)	684,644 (34,232)	890,873 (29,696)	537,593 (19,200)	
<i>N°. of brake mass spectra (per day)</i>	-	5364 (1341)	2650 (442)	5772 (1,443)	6583 (10,533)	6846 (342)	2673 (89)	2150 (78)	
<i>Total n°. clusters</i>	10	15	19	16	7	14	18	18 <sup>†</sup>	
<i>Brake dust as a percentage of dust mass spectra</i>	-	15	3.9	8.4	60	1.0	0.3	0.4	

<sup>†</sup> Analysed using *k*-Means in Enchillada (Gross et al., 2000; Giorio et al., 2012).



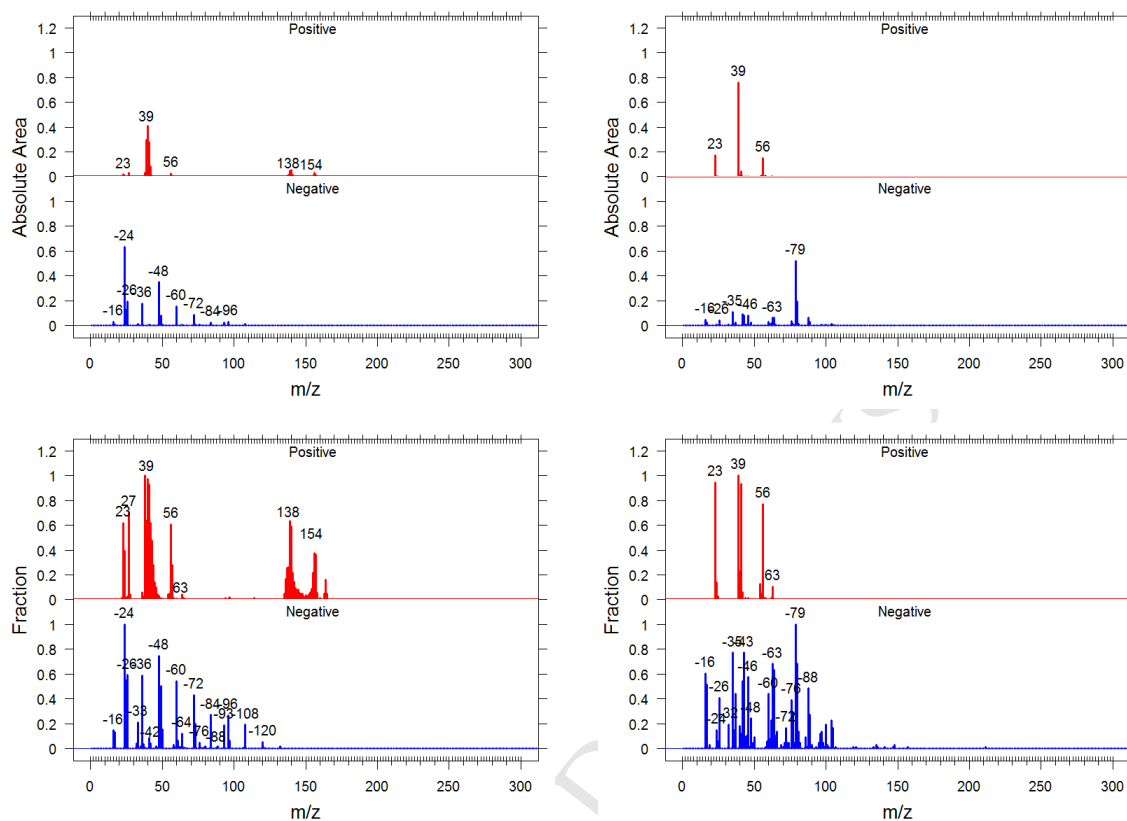
## LABORATORY ATOFMS DATA

(a) NOZZLE

(b) AERODYNAMIC LENS

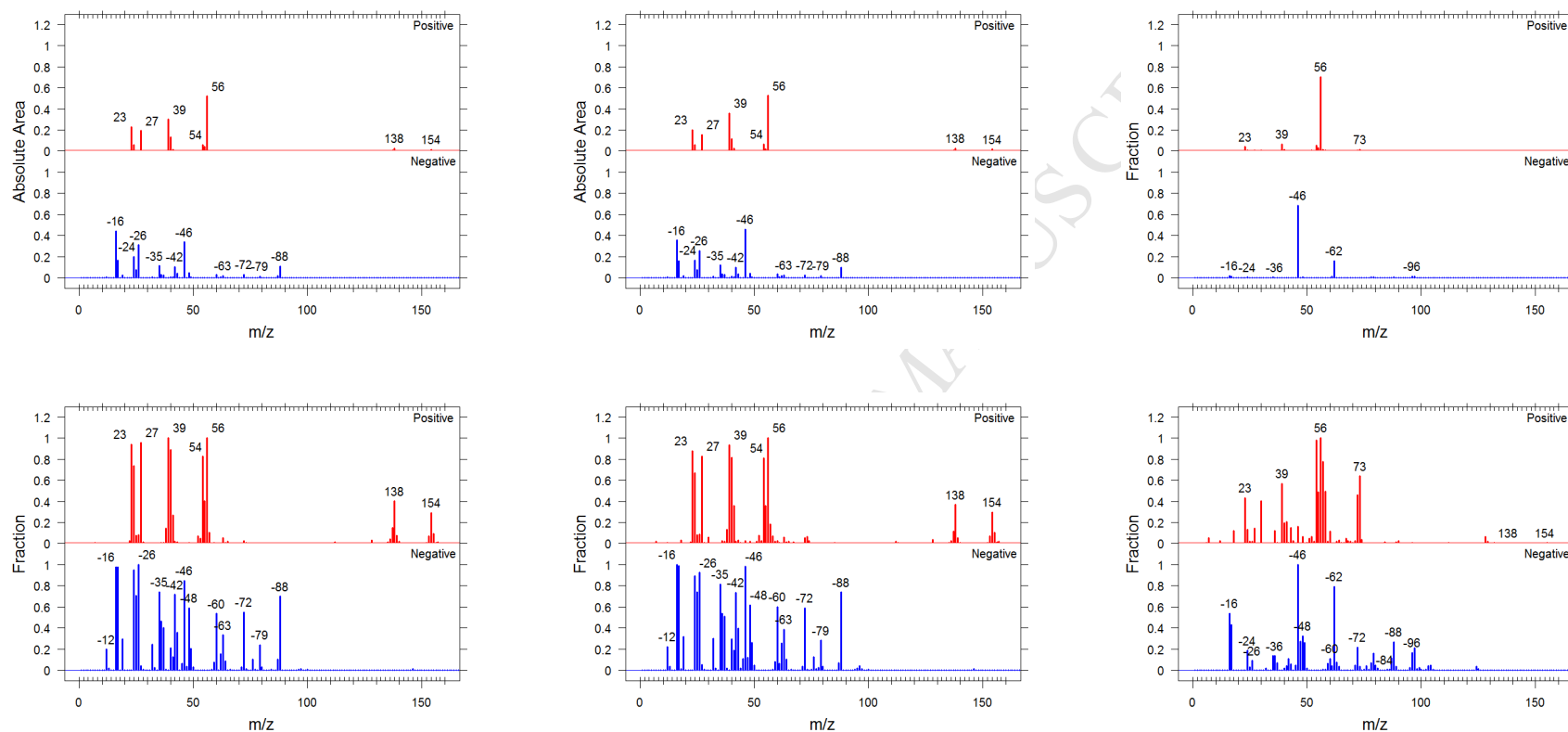
(Test Tube / 0.85mJ)

(Brake Rig / 0.19mJ)



**Figure 1:** Average mass spectra of laboratory brake dust particle clusters derived from ART2a using the nozzle inlet and 0.85 mJ laser energy (*left panels*) and AFL inlet and 0.19 mJ laser energy (*right panels*). The top graphs show ion current expressed as an absolute area of the peak. The lower graphs show the fraction of particles having the specified m/z peak.

## AMBIENT AIR ATOFMS DATA

(a) *BHAM2002 / NI*(b) *MR2009 / AFL*(c) *BCN 2010 / AFL*

**Figure 2:** Average mass spectra of ambient brake dust particle clusters derived from ART2a using the nozzle inlet (*left panels* and 0.82 mJ laser energy *BHAM2002*) and AFL inlet (*middle panels* and 0.79 mJ laser energy *MR2009* and *right panels* 0.74 mJ *BCN2010*). The upper and lower panels are generated as in Figure 1 and *BHAM2002* represents the average of *BR2002* and *QW2002*



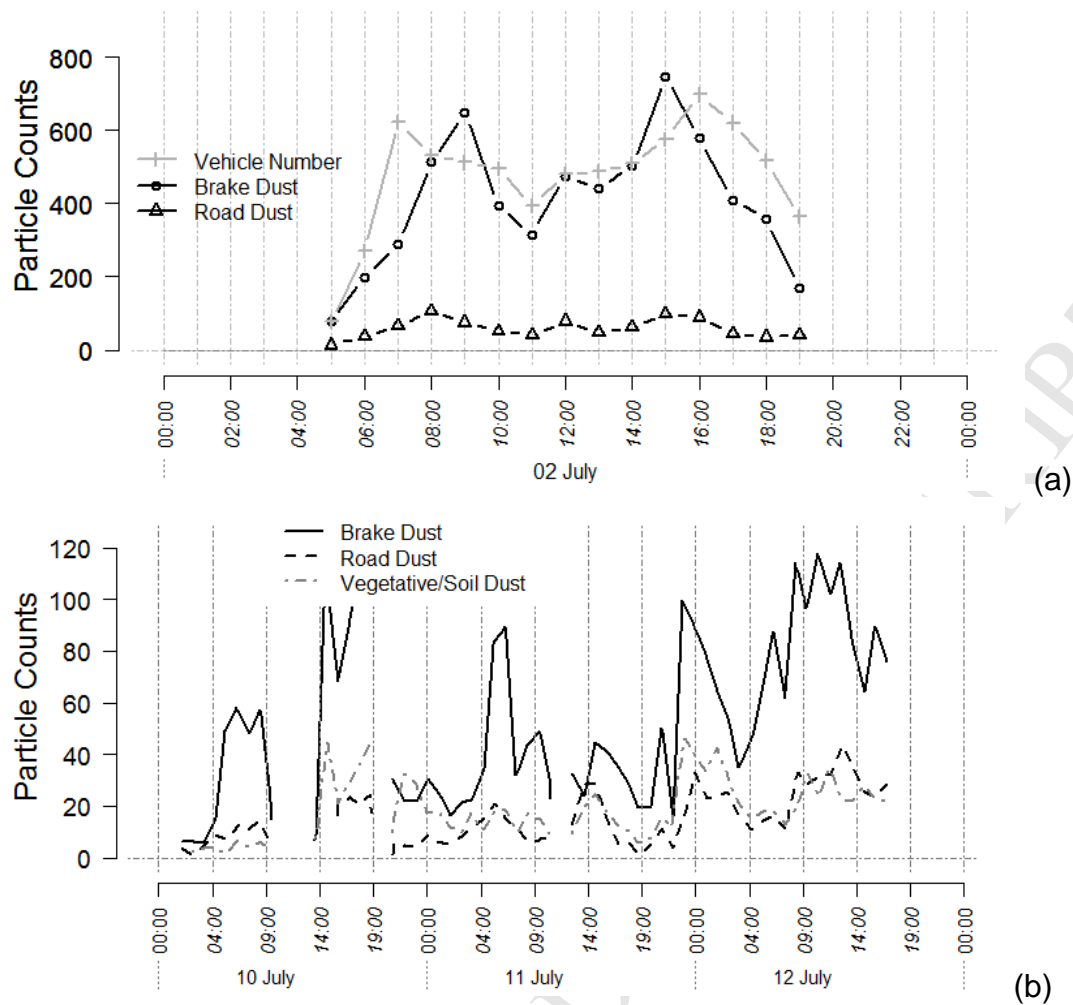


**Figure 3: (a)** Temporal trend of unscaled ATOFMS counts for brake dust and road dust along with number of vehicles detected during the Tunnel experiment (hourly resolution); **(b)** Time series of three dust types.